Check for updates

Original Article

Journal of Intelligent Material Systems and Structures

Journal of Intelligent Material Systems and Structures
2019, Vol. 30(20) 3124–3135
© The Author(s) 2019
Article reuse guidelines:
sagepub.com/journals-permissions
DOI: 10.1177/1045389X19879998
journals.sagepub.com/home/jim
SAGE

Effects of selectively triggered photothermal particles on shape memory polymer composites: An investigation on structural performance, thermomechanical characteristics and photothermal behaviour

Madhubhashitha Herath[1,2], Jayantha Epaarachchi[1,2], Mainul Islam[1,2], Cheng Yan[3], Fenghua Zhang[4] and Jinsong Leng[4]

Abstract

Light-activated shape memory polymer composites (LASMPCs) have the ability to facilitate breakthrough technological advancements in aerospace and space engineering applications since the shape memory effect can be remotely controlled by a light beam. Introduction of rare-earth organic complexes–based photothermal fillers such as Nd(TTA)$_3$Phen and Yb(TTA)$_3$Phen into thermally activated shape memory polymers has been reported as a convenient and commercially available approach to prepare light-activated shape memory polymer composites. Such light-activated shape memory polymer composites undertake selective photothermal stimulation due to light and applicable for macroscale and microscale applications. This article presents the effects of added rare-earth organic complexes of Nd(TTA)$_3$Phen and Yb(TTA)$_3$Phen, as well as glass fibre reinforcements on structural performance and shape memory behaviour of light-activated shape memory polymer composites. The physical and mechanical properties, as well as thermomechanical, shape memory, and photothermal behaviours, were systematically investigated. It has been found that the combination of photothermal fillers and glass fibre reinforcements has enhanced the capacity of light-activated shape memory polymer composites to apply for a wider range of large-scale engineering applications.

Keywords

Shape memory polymer composites, light stimulus, thermomechanical properties, photothermal effect, rear earth materials

1. Introduction

The shape memory polymers (SMPs) are capable of keeping a temporary shape and then recovering the original shape once subjected to a particular external stimulus (Herath et al., 2018). Advantageously, light-stimulated shape memory polymer composites have the capability of remote-controlled activation as the light can travel a long distance even without a medium. In addition, localized activation can be performed as the light can be focused on a certain area (Fang et al., 2017a; Herath et al., 2018). Recently, a few researchers have successfully introduced photothermal fillers into thermally activated SMPs in order to prepare light-activated shape memory polymer composites

[1]School of Mechanical and Electrical Engineering, Faculty of Health, Engineering and Sciences, University of Southern Queensland, Toowoomba, QLD, Australia
[2]Centre for Future Materials, University of Southern Queensland, Toowoomba, QLD, Australia
[3]School of Chemistry, Physics and Mechanical Engineering, Queensland University of Technology, Brisbane, QLD, Australia
[4]Center of Composite Materials and Structures, Harbin Institute of Technology, Harbin, China

Corresponding author:
Jayantha Epaarachchi, School of Mechanical and Electrical Engineering, Faculty of Health, Engineering and Sciences, University of Southern Queensland, Toowoomba, QLD 4350, Australia.
Email: Jayantha.Epaarachchi@usq.edu.au

(LASMPCs) (Fang et al., 2017a). Under irradiation, the photothermal fillers absorb light energy and transfer it into heat, which indirectly increases the temperature of the composite. Due to photothermal heating, the shape recovery occurs when the temperature reaches the glass transition temperature (T_g) (Fang et al., 2017a; Herath et al., 2018). Moreover, light is not only a form of energy but also can be presented in a signal manner for controlled actuation (Fang et al., 2017a). Photothermal fillers such as gold nanoparticles, carbon nanotubes, carbon black, carbon fibres and rare-earth organic complexes responsive to different light wavelengths, including ultra-violet light (UV), visible light and infrared light (IR), have been explored to produce LASMPCs (Mu et al., 2018). Among all such fillers rare-earth organics complexes of $Nd(TTA)_3Phen$ and $Yb(TTA)_3Phen$ have demonstrated selective photothermal effect to near-infrared (NIR) light of 808 and 980 nm, respectively (Fang et al., 2017a). The development of photothermal fillers, which are selectively responsive to a certain wavelength of light, will cause successive multishape changes of polymers to be used in smart actuators or structures (Fang et al., 2017a).

Rare-earth materials are a special group of elements in the periodic table. The term 'rare earths' has been historically applied to the lanthanides because it was originally believed that these elements were sporadically distributed in nature. Lanthanide elements (referred to as Ln) have atomic numbers that range from 57 to 71. They are lanthanum (La), cerium (Ce), praseodymium (Pr), neodymium (Nd), promethium (Pm), samarium (Sm), europium (Eu), gadolinium (Gd), terbium (Tb), dysprosium (Dy), holmium (Ho), erbium (Er), thulium (Tm), ytterbium (Yb) and lutetium (Lu). With the inclusion of scandium (Sc) and yttrium (Y), which are in the same subgroup, these 17 elements are referred to as the rare-earth elements (Huang and Bian, 2010). Interestingly, the rare-earth organic complexes have the technical versatility for various applications such as light activation of SMPs (Fang et al., 2017a), energy harvesting, ultraviolet light detection, temperature sensing, laser (Shahi et al., 2015) and light-emitting diodes (Shahalizad et al., 2017). The introduction of rare-earth ions or their complexes into polymer matrix has been carried out for few decades. In general, there are four methods for preparing rare-earth-fabricated polymers termed as blending, polymerization, sol–gel methods and solution mixing, which can be more simply classified as chemical and physical incorporations (Yan, 2017). In this study, Nd-based and Yb-based rare-earth organic complexes have been mixed into SMP epoxy using the solution cast method.

The main drawback of SMPs to use in a wider range of engineering applications is their relatively low mechanical properties and stress recovery abilities. As such, SMPs need to be reinforced before using for engineering applications (Al Azzawi et al., 2017; Herath et al., 2018). Different types of fibre reinforcements and fillers such as glass fibres (Al Azzawi et al., 2017; Ohki et al., 2004), carbon fibres (Guo et al., 2015; Herath et al., 2018), carbon nanotubes (Sahoo et al., 2007) and graphene (Meng et al., 2017) have been used to improve the mechanical properties of SMPs. Moreover, such reinforcements have been benefitted to obtain robust recovery capability under constrained conditions (Al Azzawi et al., 2018; Meng et al., 2017; Xie et al., 2018). Also the reinforcements will enhance the storage modulus and the glass transition temperature which will be advantageous for using SMP at extreme temperatures (Al Azzawi et al., 2017).

Polymer composites consist of either a thermoset or thermoplastic polymer, along with filler particles, continuous fibres or short fibres. The thermoplastic polymers act as a fluid above a certain temperature level, but the heating of a thermoset can reach higher temperatures, which leads to its degradation without going through a fluid state. Moreover, thermosets are cost effective, have high level of dimensional stability and thin to thick wall manufacturing capabilities compared to thermoplastics (Pascault, 2002). Due to this reason, a thermoset SMP epoxy has been used in this research. 0/90 woven roving plain glass fibre has been used as the reinforcement material. Particulate-reinforced shape memory polymer composites (SMPCs) demonstrate higher recovery stress and high recovery strain. However, fibre-reinforced SMPCs are widely being used as a structural material because of their relatively higher mechanical properties and recovery stresses (Al Azzawi et al., 2018; Guo et al., 2015). SMPCs are subjected to heating during its operation, which affects the dimensional stability of the components (Al Azzawi et al., 2017). Furthermore, SMPCs can be subjected to shear during its operation. Advantageously, the 0/90 woven fibre reinforcement is useful to overcome such problems (Cao et al., 2008; Ekşi and Genel, 2017). It is reported that carbon fibre–reinforced SMPCs can exhibit a robust shape recovery performance under resistant conditions (Xie et al., 2018). However, carbon fibres also absorb light energy, which will eliminate the selective triggering of LASMPCs to a particular wavelength of light (Herath et al., 2018). Therefore, glass fibre reinforcements will be more appropriate for selectively triggered LASMPCs. The photothermal fillers based on rare-earth organic complexes of $Nd(TTA)_3Phen$ and $Yb(TTA)_3Phen$, which have been used in this research, were introduced by Fang et al. (2017a). These two photothermal fillers have demonstrated selective light absorbance capabilities. Moreover, it is reported that the $Nd(TTA)_3Phen$ and $Yb(TTA)_3Phen$ are thermally stable until 270°C. From 270°C to 350°C, the ligand TTA and from 440°C to 500°C the ligand Phen will be decomposed in two steps (Fang et al., 2017a). Therefore, it is safe to use such fillers in LASMPCs, which may reach temperatures up to 270°C during its curing or operative stages.

In general, increased amounts of fillers or reinforcements will negatively affect the shape memory characteristics. Significantly high volume fractions of reinforcing materials tend to reduce the shape memory ability while enhancing the mechanical properties of the polymer (Mu et al., 2018). Usually, the shape fixity ratio decreases due to the fibre reinforcement, as fibre elasticity causes a spring-back effect during the unloading step of the shape programming process (Al Azzawi et al., 2017; Murugan et al., 2017; Nishikawa et al., 2012). Therefore, it is essential to investigate the effects of reinforcements on shape memory behaviour, and SMPC's ability to keep a temporary shape and memorize the original shape. Unfortunately, selectively triggered LASMPCs with increased mechanical properties have not introduced in order to develop large-scale engineering applications such as deployable or reconfigurable structures. Moreover, the shape memory behaviour and mechanical properties of such LASMPCs need to be quantified, which is essential to develop reliable and accurate engineering applications such as deployable satellites, space habitats and rovers for space exploration works. In this study, neat SMP, glass fibre–reinforced (GFR) SMPCs and LASMPCs with different mass ratios of rare-earth organic complexes of Nd(TTA)$_3$Phen and Yb(TTA)$_3$Phen as well as glass fibre reinforcements have been evaluated. The shape memory and structural performance of eight different samples were tested and the effects of added rare-earth organic complexes and glass fibres on each response have been systematically investigated. Moreover, potential future applications of fibre-reinforced selectively triggered LASMPCs are deliberated.

2. Materials and experimental methods

2.1. Materials

The styrene-based shape memory epoxy resin used in this research was supplied by the Harbin Institute of Technology (HIT), China. The detailed chemical composition of the SMP matrix is proprietary to the Center for Composite Materials and Structures of HIT. The roving plain (400 g/m^2) glass fibre was supplied by Changzhou Jlon Composite Co., Ltd, China. Sigma Aldrich, Australia has supplied $NdCl_3 \cdot 6H_2O$, $YbCl_3 \cdot 6H_2O$, TTA and Phen.

2.1.1. Preparation of photothermal fillers. The rare-earth organic complexes of Nd(TTA)$_3$Phen and Yb(TTA)$_3$ Phen have been prepared using co-precipitation method. First, 1 mmol of $NdCl_3 \cdot 6H_2O$ or $YbCl_3 \cdot 6H_2O$, 3 mmol TTA and 1 mmol Phen were dissolved in ethanol, respectively. Then, the ethanol solution of TTA was first added to a beaker and it was stirred at 60°C. Successively, the ethanol solution of $NdCl_3 \cdot 6H_2O$ or $YbCl_3 \cdot 6H_2O$ and the ethanol solution of Phen were added into the ethanol solution of TTA. The mixture was stirred for 15 min at 60°C. Subsequently, drops of 1 mol/L sodium hydroxide ethanol solution were added into the mixture until the pH value reaches 6–7. Afterwards, the mixture was reacted in a 60°C water bath for 6 h. Once the reaction is finished, the mixture was centrifuged at a speed of 3000 r/min for 3 h to obtain the precipitation. Then, the precipitation was dried in vacuum oven at 50°C for 12 h. Finally, the complexes were powdered using a ball mill.

Table 1. Composition of the test samples.

Sample ID	Composition
NSMP	Neat SMP
GFRSMP	4 layers of glass fibres and SMP
0.5NdSMP	0.5% Nd(TTA)$_3$Phen and SMP
1.0NdSMP	1.0% Nd(TTA)$_3$Phen and SMP
1.0NdGFRSMP	1.0% Nd(TTA)$_3$Phen, 4 layers of glass fibres and SMP
0.5YbSMP	0.5% Yb(TTA)$_3$Phen and SMP
1.0YbSMP	1.0 % Yb(TTA)$_3$Phen and SMP
1.0YbGFRSMP	1.0 % Yb(TTA)$_3$Phen, 4 layers of glass fibres and SMP

2.1.2. Preparation of LASMPCs. Eight different test samples have been prepared as shown in Table 1. Each sample was given a code according to its composition. After adding the photothermal fillers into SMP resin, the solution has been stirred for 15 min at 30°C followed by ultrasound sonication for 10 min at 30°C under 80 W ultrasound power. The neat SMP epoxy or the SMP epoxy mixed with photothermal fillers were poured in to a mould, which is prepared using two glass sheets. Inner surfaces of the glass sheets were covered with a peel fly for easy removal of the samples. In addition, four layers of glass fibres were inserted only for the samples with reinforcement. Subsequently, those moulds were kept in the oven for 9 h at 80°C, 100°C and 150°C, respectively, with equal time spacing, where the curing has taken place. Successively, eight different sheets of 300 × 300 × 2.5 mm^3 were prepared. Using a diamond saw, the sheets were cut into standard test specimens as presented in Table 2.

2.2. Experimental methods

2.2.1. Morphology. The morphology of the samples has been investigated using a Jeol Benchtop Scanning Electron Microscope (JCM-6000 SEM). Cross sections along the thickness have been observed to recognize the particle distribution and reinforcement. Moreover,

Table 2. Specification of the test specimens.

Experiment	Dimension (mm)		
	Length	Width	Thickness
DMA tests	60	8	2.5
Tensile test	250	15	2.5
Compression test	140	12.8	2.5
Impact test	100	12	2.5
Photothermal test	100	100	2.5

DMA: dynamic mechanical analysis.

using a Shimadzu Fourier Transform Infrared Spectrometer (IRAffinity-1S FTIR), the transmittance spectra of the two different photothermal fillers have been compared with the similar spectra published by Fang et al. (2017a), for the same two types of photothermal fillers.

2.2.2. UV-Vis-NIR spectroscopy. Using an Agilent Cary 5000 UV-Vis-NIR spectrophotometer, the light absorbance capacity of the pristine SMP epoxy, glass fibres and rare-earth organics complexes have been investigated.

2.2.3. Dynamic mechanical analysis. TA instruments dynamic mechanical analyzer (DMA Q800) with a double cantilever clamp has been used to investigate the thermomechanical behaviour. The multi-frequency strain mode has been used to determine the T_g and to characterize the storage modulus, using a frequency of 1 Hz and temperature ramp of 5°C/min from 35°C to 120°C. In addition, the stress-free strain recovery characteristics of the material have been investigated. The shape programming has been carried out using the following DMA programme. Under the DMA strain rate mode, the initial temperature and strain were set to 30°C and 0%, respectively. The shape programming phase was started with a temperature ramp of 5°C/min up to 100°C with zero strain, continued by a constant temperature of 100°C for 10 min with an intermediate strain ramp of 0.5%/min up to 1.5% strain. Next, the specimen was cooled with a temperature ramp of 5°C/min down to 30°C while keeping the 1.5% constant strain. Subsequently, the specimen was kept at a constant temperature of 30°C for 10 min and the constraint was released where the temporary fixed shape was achieved. The stress-free strain recovery has been investigated under DMA strain rate mode. The preprogrammed specimens were subjected to a temperature ramp of 5°C/min up to 100°C and isothermal for 10 min where the strain recovery was observed.

2.2.4. Mechanical and physical properties. The mechanical properties of the material have been examined to ensure structural performance in robust conditions. MTS 100 kN, Insight Electromechanical Testing Systems has been used for the tensile testing. Furthermore, compression testing was carried out on the same MTS testing machine. The impact testing has been performed using an Instron Dynatup Drop Weight Impact Testing Instrument (8200). SCHMIDT Shore Durometer HPSC has been used to determine the hardness of the polymer material. All experiments have been conducted at room conditions. Surface roughness of the test samples was investigated using the MarSurf M 400 Surface Measuring Instrument. In addition, the density of the test samples was examined.

2.2.5. Photothermal effect. The samples 1.0NdGFRSMP and 1.0YbGFRSMP (GFR LASMPCs) were exposed to three different power densities (1, 2, 3 W/cm^2) of NIR radiation of 808 and 980 nm, respectively, and the respective photothermal behaviour have been investigated using a FLIR A65 thermal imaging camera. The samples were exposed to a 10 mm-diameter circular laser area and the temperature variations were recorded and plotted for a 3×3 pixels region at the centre of the laser exposed area.

3. Results and discussion

3.1. Material

Figure 1(a) shows the two types of photothermal particulate fillers used to prepare the LASMPCs. As illustrated in Figure 1(b), the FTIR transmittance spectra of the two different photothermal fillers have been investigated and compared with the similar spectra published by Fang et al. (2017a). Table 3 describes the characteristic bands identified by Fang et al. (2017a) and associated comparison with the rare-earth organic complexes used in this research. Accordingly, the chemical structures of the Nd(TTA)$_3$Phen and Yb(TTA)$_3$ Phen used in this research are very nearly similar to the photothermal fillers introduced by Fang et al. (2017a).

3.1.1. Light absorbance. In order to identify the light absorbance capabilities of the raw materials, which were used to prepare the LASMPCs, the UV-Vis-NIR spectroscopy has been carried out. Figure 2 shows the transmittance spectra ranging from 200 to 1200 nm. Accordingly, both Nd(TTA)$_3$Phen and Yb(TTA)$_3$ Phen have demonstrated absorbance of UV radiation up to 380 nm, visible light from 420 to 490 nm and NIR radiation from 1099 to 1115 nm, which may be attributed to the absorbance of the ligands (Shahalizad et al., 2017). The rare-earth organic complex of Yb(TTA)$_3$Phen has presented a unique NIR absorbance capability starting at 888 nm and ending at 1063 nm, where the peak is from 940 to 980 nm. The Nd(TTA)$_3$Phen has demonstrated unique absorbance

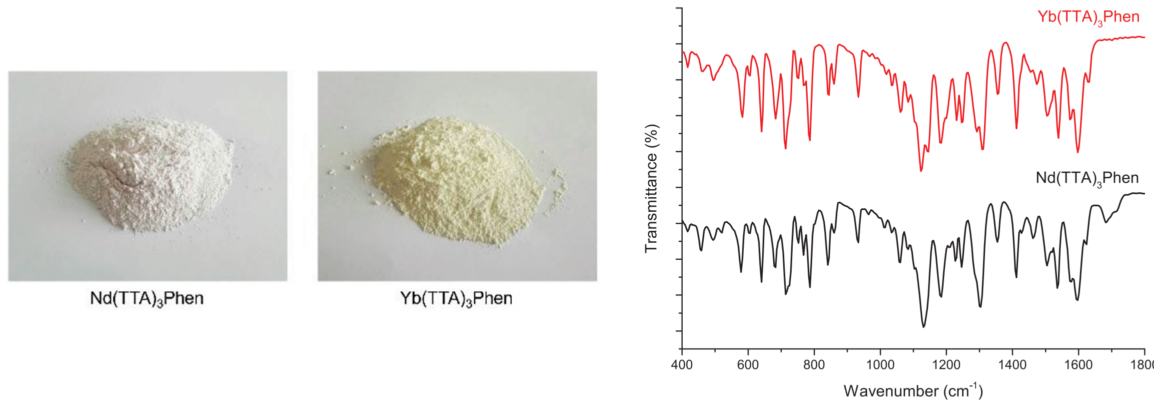

(a) (b)

Figure 1. Photothermal fillers Nd(TTA)$_3$Phen and Yb(TTA)$_3$Phen: (a) physical appearance and (b) FTIR transmittance spectra.

peaks around visible light of 527, 581 and 683 nm as well as NIR radiation of 748 and 801 nm. The glass fibres and neat SMP epoxy have shown a light absorbance capability in the UV range. However, both glass fibres and neat SMP epoxy have not demonstrated significantly intensive band of light absorbance peaks. Therefore, incorporation of Nd(TTA)$_3$Phen and Yb(TTA)$_3$Phen into GFR SMP epoxy will facilitate selectively triggered photothermal effect. In comparison to UV light, NIR light beam is relatively safe for human bodies and naked eyes (Fang et al., 2017b). Moreover, UV radiation may result in material degradation and affect the shape memory effect (Al Azzawi et al., 2018). The noticeable drawback of NIR light, which cannot be overlooked, is its invisibility. However, this can be resolved by adding upconversion particles (Fang et al., 2017b).

3.1.2. Morphology. Figure 3(a) to (d) illustrate the SEM images of the cross sections of neat SMP, SMPC with photothermal fillers, GFR SMPC and GFR SMPC with photothermal fillers, respectively. Accordingly, it is revealed that the SMPC with photothermal fillers shown in Figure 3(b) contains microlevel voids at few locations compared to the neat SMP shown in Figure 3(a). However, as shown in Figure 3(d), the GFR SMPC with photothermal fillers has demonstrated improved aspects of fibre bonding and adhesion between fibre and matrix. Under loaded circumstances, the poor bonding between the fibre and matrix will cause local bending to propagate microdelamination until the failure (Herath et al., 2018; Kakei et al., 2017). Accordingly, the GFR SMPCs with photothermal fillers have a less possibility for a delamination failure while operating with loads. Moreover, as shown in Figure 3(b) and (d), the SMPCs with photothermal fillers and GFR SMPCs with photothermal fillers have demonstrated uniform surface features throughout the cross section, which indicates that the particulate photothermal fillers have been incorporated into the SMP matrix in homogeneous manner.

3.2. Mechanical and physical properties

Inherent poor mechanical properties of neat SMP cause limitation of its applications in large-scale engineering structures. The inclusion of fibres improves the mechanical properties of SMPCs significantly. However, inclusion of rare-earth organic complexes–based photothermal fillers into SMP and GFR SMPC affects the mechanical and physical properties of the parent SMP or SMPC material. Due to this reason, the eight different test samples, which are described in Table 1, were systematically investigated. Figure 4(a) shows the tensile behaviour of the test specimens. The neat SMP has shown an ultimate tensile strength (UTS) of 48 MPa, which has increased up to 181 MPa once reinforced with glass fibres. However, the inclusion of rare-earth organic complexes–based particles has reduced the UTS of the SMPCs (without fibres) compared to the neat SMP. The SMPCs with photothermal fillers have demonstrated a higher ductility and plastic deformation over 0.25% strain. At any strain level, the stress exhibited by a cross-linked network system is related to the crosslink density as given by the theory of rubber elasticity. The elastic modulus decreases as the crosslink density decreases (Mukherjee et al., 1976). It has been noted that the UTS of the SMPCs have been increased slightly with respect to the increase of photothermal filler materials. The reason for such increment in UTS is the increase of cross-linked density due to the higher levels of ligand TTA and ligand Phen. Furthermore, the SMPCs with Yb(TTA)$_3$Phen have demonstrated a higher UTS compared to the SMPCs with similar mass percentage of Nd(TTA)$_3$Phen. The incorporation of glass fibres has been advantageous to improve the UTS of the SMPCs

Table 3. Characteristic FTIR bands of Nd(TTA)$_3$Phen and Yb(TTA)$_3$Phen.

Common FTIR bands identified by Fang et al. (2017a) for Nd(TTA)$_3$Phen and Yb(TTA)$_3$Phen (cm^{-1})	FTIR bands of the materials used in this research (cm^{-1})		Remarks
	Nd(TTA)$_3$Phen	Yb(TTA)$_3$Phen	
1601	1597	1597	Due to the Vc = o stretching (1642 and 1661 cm^{-1}) of TTA (Fang et al., 2017a; Zhao et al., 2006)
1625	1625	1631	
1536	1537	1541	Due to the characteristic ring stretching vibration bands (1563, 851 and 736 cm^{-1}) of Phen (Fang et al., 2017a; Zhao et al., 2006)
842	840	844	
715	713	713	

FTIR: Fourier transform infrared spectroscopy.

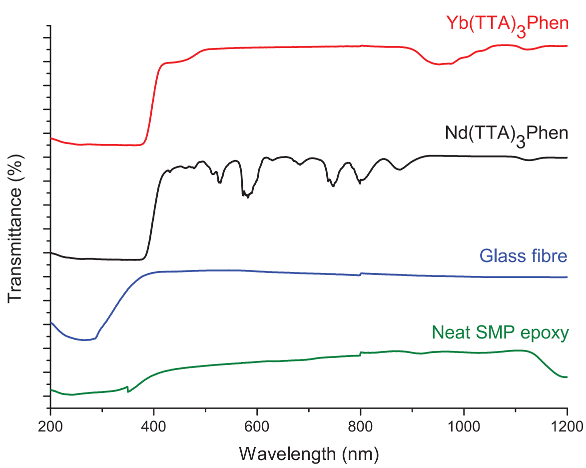

Figure 2. UV-Vis-NIR transmittance spectra of the raw materials used to prepare LASMPCs.

with rare-earth organic complexes–based photothermal fillers. The GFR SMPCs with 1% of Nd(TTA)$_3$Phen and Yb(TTA)$_3$Phen have demonstrated an UTS of 124 and 164 MPa, respectively, which exhibit a significant improvement compared to the SMPCs only with photothermal particles.

Figure 4(b) shows the uniaxial compression test results. Accordingly, the neat SMP and GFR SMPC have demonstrated compression strength of 82 and 185 MPa, respectively. Inclusion of rare-earth organic complexes–based fillers has reduced the compression strength of the SMPCs. Even though the SMPCs with photothermal fillers have been reinforced with glass fibres, those samples do not show a significant improvement in compressive strength. As illustrated in Figure 5, the buckling behaviour demonstrated by the SMPCs with photothermal fillers (with and without glass fibres) under uniaxial compression loading has caused the reduced compression properties of those SMPCs. Buckling is generally avoided during design modifications. Buckling has been a major concern in the design of all slender structural elements due to the resultant capacity reduction associated with large deformations and the resultant catastrophic failure. However, the increasing interest in the design of smart devices and mechanical components has identified buckling and post-buckling response as a favourable behaviour (Hu and Burgueño, 2015). Therefore, the enhanced buckling behaviour of SMPCs due to the inclusion of rare-earth organic complexes–based particulate fillers will be advantageous to develop the energy- and motion-related smart applications activated by light (Hu and Burgueño, 2015).

The recent progresses of SMP research have been focused to develop SMPC-based space engineering applications (Liu et al., 2014). However, remaining stable in the presence of micrometeoroids and space debris are the challenging concerns on selecting lightweight materials for space applications. Therefore, the SMPCs with improved impact energy absorbance will be a major requirement. Figure 4(c) illustrates the impact energy absorbance and hardness of the test specimens. Inclusion of 0.5% of rare-earth organic complexes into SMP network has doubled the impact energy absorbance of the SMPCs. However, the inclusion of 1% of rare-earth organic complexes has not shown any improved impact energy absorbance compared to the neat SMP. The reason for that might be the increase in microlevel voids or barriers that reduce the cross-linking due to the higher levels of particulate fillers. Interestingly, the GFR SMPCs have shown a significant improvement in impact energy absorbance compared to neat SMP and SMPCs only with photothermal fillers. The inclusion of rare-earth organic complexes has reduced the hardness of the SMPCs. In engineering point of view, hardness is an important factor as the resistance to wear due to friction or erosion depends on the hardness of the material. The glass fibre reinforcements have relatively improved the hardness of the SMPCs.

Figure 4(d) illustrates the surface roughness and density of the test specimens. The surface roughness of LASMPCs is an important factor to be considered. According to Beer–Lambert law the light absorption of a specimen depends on three variables called extinction coefficient, path length and concentration of the substance (Swinehart, 1962). The extinction coefficient,

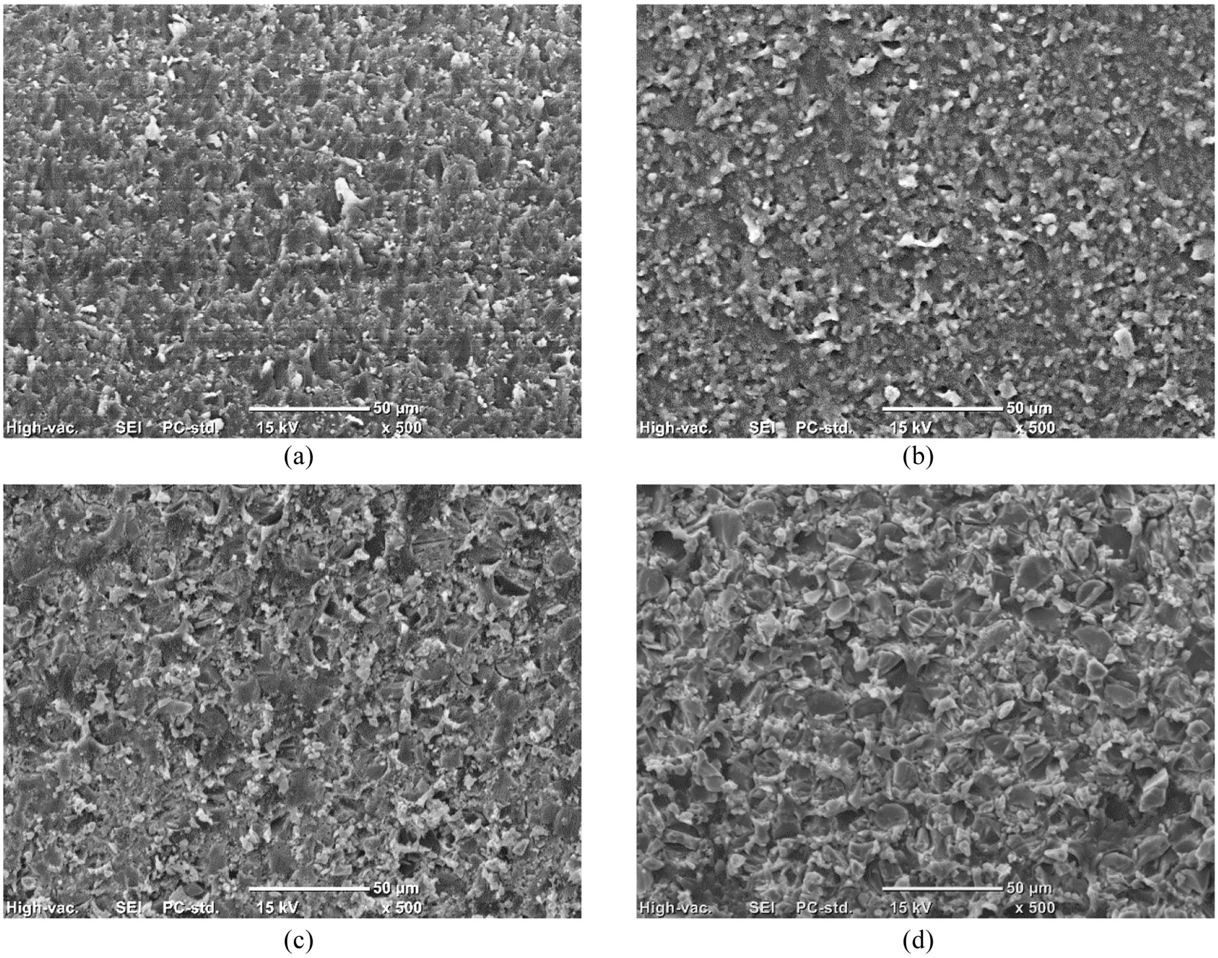

Figure 3. SEM images of the cross sections of (a) neat SMP, (b) SMPC with photothermal fillers, (c) GFR SMPC and (d) GFR SMPC with photothermal fillers.

which is also known as absorptivity, depends on the material and its surface. As the surface roughness increases, the surface reflectance decreases, which enables penetration of more light into the substance. Interestingly, the inclusion of rare-earth organic complexes–based fillers has enhanced the surface roughness of the SMPCs compared to its parent SMP material. Furthermore, the glass fibre reinforcements have enhanced the surface roughness significantly. The inclusion of rare-earth organic complexes–based particles has increased the density of the SMPCs. Moreover, an increment in density has been shown due to the glass fibre reinforcements.

3.3. Thermomechanical characteristics

According to Baghani et al. (2012), below T_g a material is at dominant frozen phase and above T_g a material is at dominant active phase. At a certain range around T_g, a material demonstrates combined properties of both phases, where the shape changes occur (Baghani et al., 2012). Here, the T_g is defined by considering the peak of the tan delta curve shown in Figure 6(a). The neat SMP and GFR SMPC have demonstrated a T_g of 99°C and 91°C, respectively. Inclusion of rare-earth organic complexes has reduced the T_g of the SMPCs, which lies between 58°C and 62°C. The samples with lesser amount (0.5%) of photothermal fillers have demonstrated lower T_g. Once the amount of photothermal fillers has increased (1.0%), the T_g has increased slightly. Furthermore, $Yb(TTA)_3Phen$-incorporated samples have shown a higher T_g than the samples incorporated with the same amount of $Nd(TTA)_3Phen$. Inclusion of glass fibres has reduced the T_g of the samples compared to their parent material. The SMPCs with higher T_g will be appropriate for structural engineering applications as the shape memory activation will not take place due to the environmental temperature changes. In that case, the SMPCs incorporated with rare-earth organic complexes–based photothermal fillers may require a thermal insulation coating, which can transmit the NIR light.

Figure 6(b) illustrates the storage modulus curves of the tested samples. The storage modulus represents the

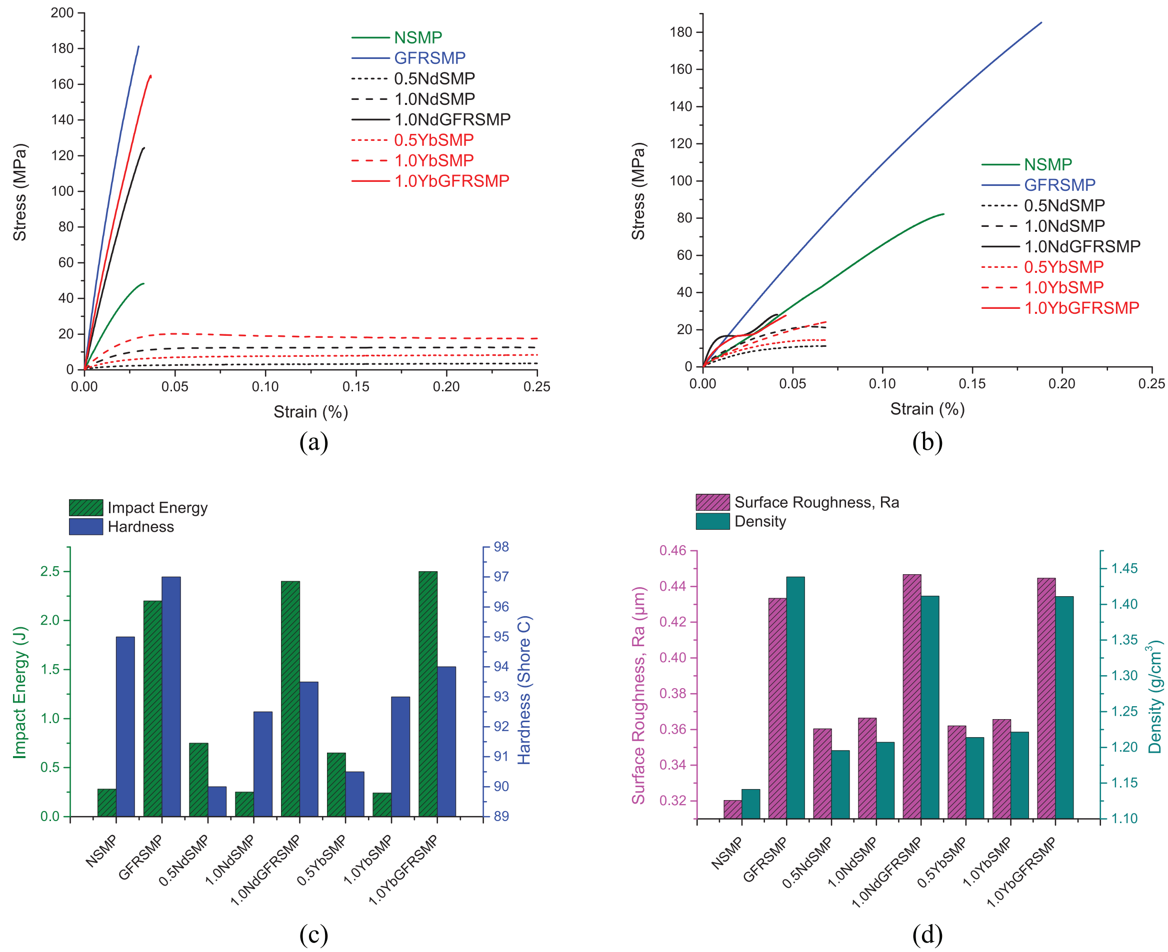

Figure 4. Mechanical and physical properties: (a) tensile stress versus strain, (b) compression stress versus strain, (c) impact energy and hardness and (d) surface roughness and density.

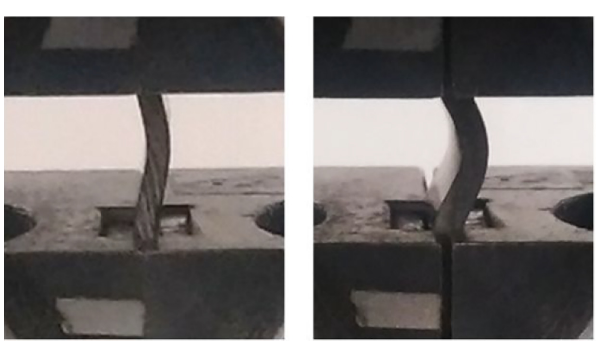

Figure 5. Buckling behaviour demonstrated by the SMPCs with photothermal fillers under uniaxial compression loading.

capability of energy storage in elastic manner. All specimens have shown a higher storage modulus at lower temperatures and critically low modulus at higher temperatures. This happens due to the entropy elasticity caused by the micro-Brownian movement in rubbery phase (Al Azzawi et al., 2017; Ohki et al., 2004). The inclusion of glass fibre reinforcements into SMP matrix has demonstrated a significant improvement in storage modules. However, the samples incorporated with rare-earth organic complexes–based photothermal fillers have shown a reduced storage modulus compared to the parent SMP material. Even though the SMPCs with photothermal fillers are reinforced with glass fibres, no improvement in storage modulus has been demonstrated. The SMPCs with lower storage modulus will not be appropriate for shape memory activation under applied load. However, most of the space engineering applications require shape memory activation with zero or low loads, as the gravity at space is insignificant.

3.4. Shape memory behaviour

The strain recovery curve obtained from DMA, under strain rate mode (stress free condition), presents the shape fixity and recovery characteristics. Accordingly, the DMA strain recovery curves were obtained and presented in Figure 7. For clear representation, the full shape memory cycle has been divided into two parts.

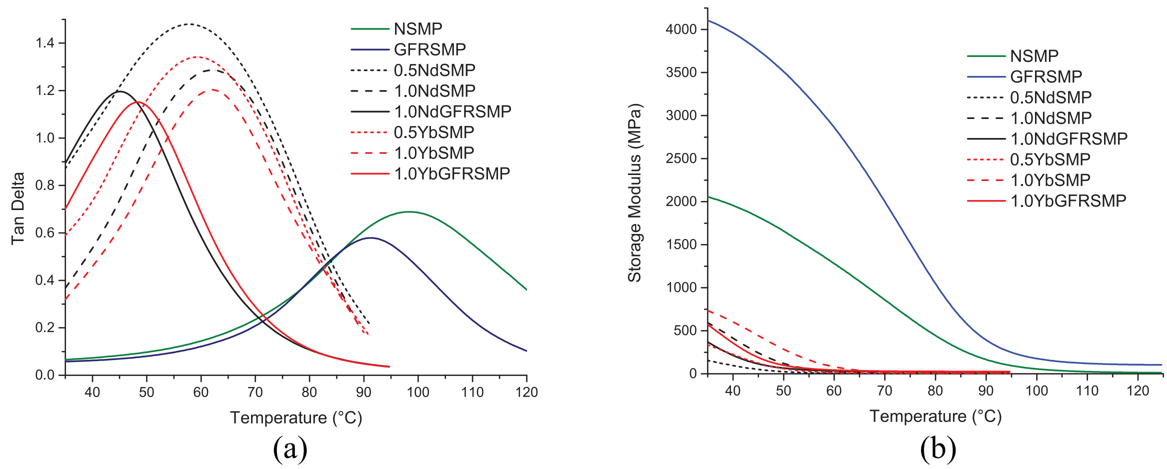

Figure 6. Thermomechanical behaviour: (a) tan delta and (b) storage modulus.

Figure 7(a) illustrates the first half of the shape memory cycle, which is shape fixing common for all test samples. Accordingly, the samples were programmed into a 1.5% strain at 100°C. Afterwards the samples were cooled down to 30°C and load was removed. In the second half of the shape memory cycle, which is shape recovery, the samples were heated up to 100°C and set isothermal for 10 min. Figure 7(b) illustrates the shape recovery behaviours of each test sample. The recovery rate, shape fixity ratio and recovery ratio defined by Fejős et al. (2012) were calculated for each test sample and presented in Table 4. Accordingly, the neat SMP has shown the highest recovery rate. Inclusion of rare-earth organic complexes has reduced the shape recovery rate compared to its parent material.

The SMPCs incorporated with both glass fibres and photothermal fillers have demonstrated a fast recovery (~0.23%/min) until 0.7% strain around their T_g. However, at higher temperatures, those SMPCs have shown further recovery at a lower rate.

The neat SMP has demonstrated an excellent shape fixity. Inclusion of photothermal fillers has reduced the shape fixity. Compared to parent material, the GFR SMPC samples have shown a lower fixity capability. The reason being the spring-back effect caused due to the fibre elasticity of the incorporated glass fibres during the unloading (Al Azzawi et al., 2017; Murugan et al., 2017; Nishikawa et al., 2012). The inclusion of rare-earth organic complexes has not demonstrated a significant effect on shape recovery ratio. The strain concentration near the fibre ends and fibre elasticity play important roles in the shape recovery properties of the SMPCs (Nishikawa et al., 2012). The GFR samples with photothermal fillers have demonstrated a lower shape recovery ratio compared to the SMPCs without fibre reinforcements.

3.5. Photothermal behaviour

The photothermal effect is a phenomenon which produces the thermal energy from electromagnetic radiation. Once the electromagnetic radiation is absorbed by a material, free electrons of the material will vibrate at very high frequency and reach higher energy levels. Part of the vibrational energy is converted into the electromagnetic waves and radiate outwards. The rest is transformed into kinetic energy of electrons and then converted into heat energy through the relaxation process between electrons and lattices (Herath et al., 2018; Liu et al., 2018). As shown in Figure 2, Yb(TTA)$_3$Phen has demonstrated a unique absorbance peak from 940 to 980 nm. Also Nd(TTA)$_3$Phen has a unique absorbance peak around 801 nm. Accordingly, two commonly used NIR lasers of 808 and 980 nm wavelengths were used to heat the GFR LASMPCs with Nd(TTA)$_3$Phen and Yb(TTA)$_3$Phen, respectively. Figure 8(a) and (b) illustrate the temperature increment for 300 s due to three different power densities (1, 2 and 3 W/cm^2) of 808 nm (irradiated to sample 1.0NdGFRSMP) and 980 nm (irradiated to sample 1.0YbGFRSMP), respectively. Both samples have reached a temperature above T_g within 300 s, once exposed to a power density of 2 W/cm^2 or higher. The increment of power density reduces the time required to reach T_g. The demonstrated photothermal behaviour will assist in NIR-triggered shape recovery of GFR LASMPCs.

Fang et al. (2017a) have introduced macro and microscale applications of such LASMPCs. The LASMPCs with Nd(TTA)$_3$Phen and Yb(TTA)$_3$Phen have been used to develop multi-shaped actuator upon the sequential irradiation of two NIR light bands. However, for large-scale engineering applications, fibre-reinforced LASMPCs are needed to maintain the

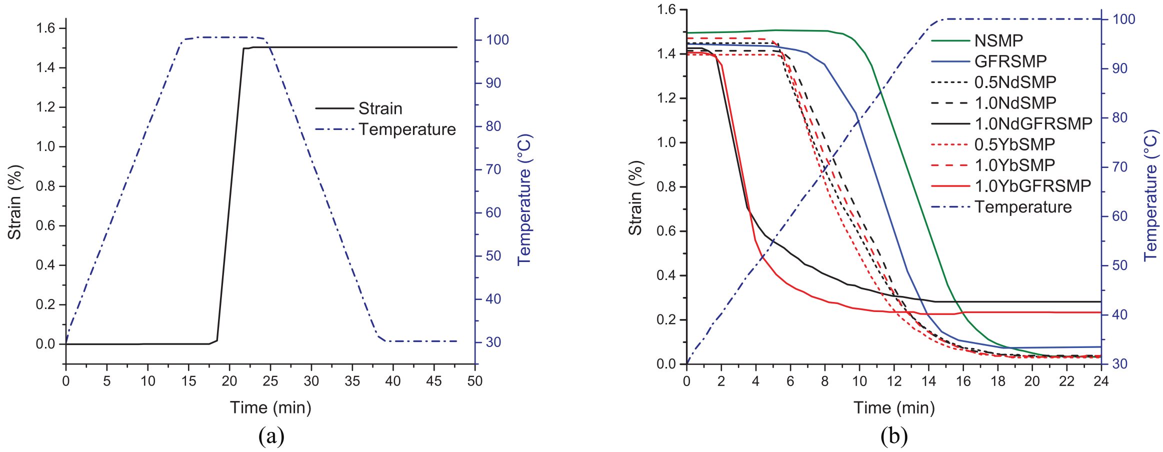

Figure 7. Shape fixity and recovery behaviour under stress free condition: (a) common shape fixing curve for all test samples and (b) shape recovery curves of the each test samples.

Table 4. Shape memory characteristics of the test samples.

Sample ID	NSMP	GFRSMP	0.5NdSMP	1.0NdSMP	1.0NdGFRSMP	0.5YbSMP	1.0YbSMP	1.0YbGFRSMP
Shape recovery rate (%/min)	0.12	0.11	0.10	0.11	0.09	0.10	0.10	0.09
Shape fixity ratio (%)	99.70	96.29	96.58	94.27	95.10	93.08	98.08	93.73
Shape recovery ratio (%)	97.05	94.52	97.69	97.41	81.21	97.40	97.45	85.03

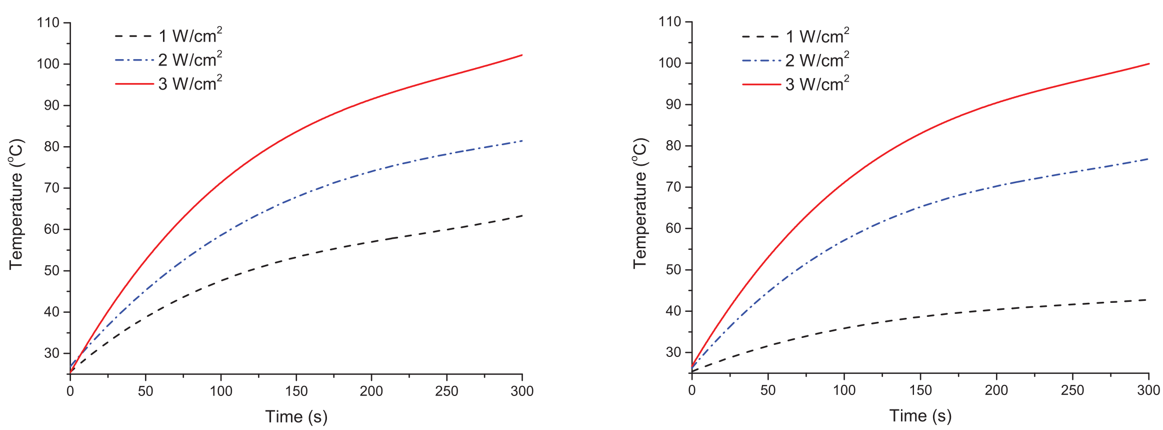

Figure 8. Photothermal behaviour due to NIR radiation: (a) 1.0NdGFRSMP sample exposed to 808 nm and (b) 1.0YbGFRSMP sample exposed to 980 nm.

required strength and the stiffness. The GFR SMPCs with selective triggering capability will be advantageous for the space engineering applications such as deployable solar arrays (Herath et al., 2018), deployable space habitats (Herath et al., 2019), deployable hinges and antennas (Liu et al., 2014). Selective light activation ability of SMP material with enhanced mechanical and physical properties will make such material suitable for advanced engineering applications. However, a thermal insulation coating will be necessary for such LASMPCs at extreme temperature environments, where the light can enter into the material through optical fibres.

4. Conclusion

This article deliberates a systematic investigation on the effects of rare-earth organic complexes–based photothermal fillers and glass fibre reinforcement on shape memory behaviour and structural performance of selectively triggered LASMPCs. Interestingly, Nd(TTA)$_3$Phen and Yb(TTA)$_3$Phen-based photothermal fillers have shown the ability of unique wavelength light absorbance, which is impossible with neat SMP and glass fibres. The inclusion of photothermal fillers has negatively affected the mechanical properties of the LASMPCs. However, the glass fibre reinforcement has increased the mechanical properties except compression strength as anticipated. Moreover, the photothermal fillers have decreased the T_g and storage modulus significantly. The shape fixity and recovery ratios were affected by the glass fibre reinforcements. The Yb(TTA)$_3$Phen-based LASMPCs have demonstrated superior performance favourable for engineering applications relative to Nd(TTA)$_3$Phen-based LASMPCs. The findings of this investigation have confirmed the ability of the fibre-reinforced LASMPCs with selective triggering capability for large-scale engineering applications.

Acknowledgements

The authors are indebted to the Harbin Institute of Technology, China, for providing help and SMP material used in this work. Furthermore, the authors appreciate the support provided by Wei Zhao at Harbin Institute of Technology and Kimal Wasalathilake at Queensland University of Technology.

Declaration of conflicting interests

The author(s) declared no potential conflicts of interest with respect to the research, authorship and/or publication of this article.

Funding

The author(s) disclosed receipt of the following financial support for the research, authorship and/or publication of this article: This work was supported by the Asian Office of Aerospace Research and Development (AOARD), Air Force Office of Scientific Research (AFOSR), U.S. Air Force (grant number FA2386-16-1-4043).

ORCID iD

Madhubhashitha Herath https://orcid.org/0000-0002-6796-0802

References

Al Azzawi W, Epaarachchi JA and Leng J (2018) Investigation of ultraviolet radiation effects on thermomechanical properties and shape memory behaviour of styrene-based shape memory polymers and its composite. *Composites Science and Technology* 165: 266–273.

Al Azzawi W, Islam MM, Leng J, et al. (2017) Quantitative and qualitative analyses of mechanical behavior and dimensional stability of styrene-based shape memory composites. *Journal of Intelligent Material Systems and Structures* 28: 3115–3126.

Baghani M, Naghdabadi R, Arghavani J, et al. (2012) A constitutive model for shape memory polymers with application to torsion of prismatic bars. *Journal of Intelligent Material Systems and Structures* 23: 107–116.

Cao J, Akkerman R, Boisse P, et al. (2008) Characterization of mechanical behavior of woven fabrics: experimental methods and benchmark results. *Composites Part A: Applied Science and Manufacturing* 39: 1037–1053.

Ekşi S and Genel K (2017) Comparison of mechanical properties of unidirectional and woven carbon, glass and aramid fiber reinforced epoxy composites. *Acta Physica Polonica A* 132: 879–882.

Fang L, Chen S, Fang T, et al. (2017a) Shape-memory polymer composites selectively triggered by near-infrared light of two certain wavelengths and their applications at macro-/microscale. *Composites Science and Technology* 138: 106–116.

Fang L, Fang T, Liu X, et al. (2017b) Precise stimulation of near-infrared light responsive shape-memory polymer composites using upconversion particles with photothermal capability. *Composites Science and Technology* 152: 190–197.

Fejős M, Romhány G and Karger-Kocsis J (2012) Shape memory characteristics of woven glass fibre fabric reinforced epoxy composite in flexure. *Journal of Reinforced Plastics and Composites* 31: 1532–1537.

Guo J, Wang Z, Tong L, et al. (2015) Shape memory and thermo-mechanical properties of shape memory polymer/carbon fiber composites. *Composites Part A: Applied Science and Manufacturing* 76: 162–171.

Herath M, Epaarachchi JA, Islam MM, et al. (2018) Structural performance and photothermal recovery of carbon fibre reinforced shape memory polymer. *Composites Science and Technology* 167: 206–214.

Herath M, Epaarachchi JA, Islam MM, et al. (2019) Carbon fibre reinforced shape memory polymer composites for deployable space habitats. *Engineer Journal of the Institution of Engineers Sri Lanka* 52: 1–9.

Hu N and Burgueño R (2015) Buckling-induced smart applications: recent advances and trends. *Smart Materials and Structures* 24: 063001.

Huang C and Bian Z (2010) Introduction. In: Huang C (ed.) *Rare Earth Coordination Chemistry: Fundamentals and Applications*. Singapore: John Wiley & Sons, pp. 1–39.

Kakei AA, Islam M, Leng J, et al. (2017) Use of an elasto-plastic model and strain measurements of embedded fibre Bragg grating sensors to detect Mode I delamination crack propagation in woven cloth (0/90) composite materials. *Structural Health Monitoring* 17: 363–378.

Liu Y, Du H, Liu L, et al. (2014) Shape memory polymers and their composites in aerospace applications: a review. *Smart Materials and Structures* 23: 023001.

Liu Y, Zhu G, Liu W, et al. (2018) An investigation on laser-triggered shape memory behaviors of hydro-epoxy/carbon black composites. *Smart Materials and Structures* 27: 095008.

Meng Z-Y, Chen L, Zhong H-Y, et al. (2017) Effect of different dimensional carbon nanoparticles on the shape memory behavior of thermotropic liquid crystalline polymer. *Composites Science and Technology* 138: 8–14.

Mu T, Liu L, Lan X, et al. (2018) Shape memory polymers for composites. *Composites Science and Technology* 160: 169–198.

Mukherjee DP, Kagan HM, Jordan RE, et al. (1976) Effect of hydrophobic elastin ligands on the stress-strain properties of elastin fibers. *Connective Tissue Research* 4: 177–179.

Murugan MS, Rao S, Chiranjeevi M, et al. (2017) Actuation of shape memory polymer composites triggered by electrical resistive heating. *Journal of Intelligent Material Systems and Structures* 28: 2363–2371.

Nishikawa M, Wakatsuki K, Yoshimura A, et al. (2012) Effect of fiber arrangement on shape fixity and shape recovery in thermally activated shape memory polymer-based composites. *Composites Part A: Applied Science and Manufacturing* 43: 165–173.

Ohki T, Ni Q-Q, Ohsako N, et al. (2004) Mechanical and shape memory behavior of composites with shape memory polymer. *Composites Part A: Applied Science and Manufacturing* 35: 1065–1073.

Pascault JP (2002) *Thermosetting Polymers*. Boca Raton, FL: CRC Press.

Sahoo NG, Jung YC, Yoo HJ, et al. (2007) Influence of carbon nanotubes and polypyrrole on the thermal, mechanical and electroactive shape-memory properties of polyurethane nanocomposites. *Composites Science and Technology* 67: 1920–1929.

Shahalizad A, D'Aléo A, Andraud C, et al. (2017) Near infrared electroluminescence from $Nd(TTA)_3phen$ in solution-processed small molecule organic light-emitting diodes. *Organic Electronics* 44: 50–58.

Shahi PK, Singh AK, Singh SK, et al. (2015) Revelation of the technological versatility of the $Eu(TTA)_3phen$ complex by demonstrating energy harvesting, ultraviolet light detection, temperature sensing, and laser applications. *ACS Applied Materials & Interfaces* 7: 18231–18239.

Swinehart DF (1962) The Beer-Lambert Law. *Journal of Chemical Education* 39: 333.

Xie H, Li L, Deng X-Y, et al. (2018) Reinforcement of shape-memory poly(ethylene-co-vinyl acetate) by carbon fibre to access robust recovery capability under resistant condition. *Composites Science and Technology* 157: 202–208.

Yan B (2017) Photofunctional rare earth hybrid materials based on polymer and polymer/silica composite. In: Yan B (ed.) *Photofunctional Rare Earth Hybrid Materials*. Singapore: Springer, pp. 135–163.

Zhao S, Zhang L, Li W, et al. (2006) Preparation and fluorescent property of $Eu(TTA)_3phen$ incorporated in polycarbonate resin. *Polymer Journal* 38: 523–526.